Closed-form solution for the three-point Dixon method with advanced spectrum modeling

J. Berglund[1], H. Ahlström[1], L. Johansson[1], and J. Kullberg[1]
[1]Oncology, Radiology and Clinical Immunology, Uppsala University, Uppsala, Sweden

Introduction The Dixon method [1] enables separation of water (*W*) and lipid (*L*) signal. The chemical shift dimension is sampled by shifting the signal readout with time *t* relative to a point where all resonances are in-phase. This happens at excitation in spoiled gradient echo, and at the spin echo in spin echo acquisitions. Commonly, three points are sampled with constant spacing Δt of the shifts.

Advanced spectrum modeling with multiple lipid spectral peaks give more accurate signal estimates, compared to single-peak modeling [2]. However, closed-form solutions have only been described for single-peak modeling [3, 4].

In this work, a closed-form solution is given for the three-point Dixon method with advanced spectrum modeling, which previously required optimization.

Methods The spectral dimension is sampled at time shifts t_n, n=(1, 2, 3) with a constant spacing Δt. In each voxel, the signal model defined by eq. 1 is used for the complex sample n. The angular frequency offset ω_0 is primarily associated with static field inhomogeneity. The known model parameters a are defined by eq. 2, where P is the number of lipid spectral peaks and TE is the echo time (=t in spoiled gradient echo acquisitions). For each peak p, the relative amount α, the angular frequency relative to water $\Delta\omega$, and $R_2 = 1/T_2$ are assumed known *a priori*. The closed-form solution for the *error phasor* is then given by eq. 3, where $c_1 = (a_{W,1}a_{L,3} - a_{W,3}a_{L,1})$, $c_2 = (a_{W,1}a_{L,2} - a_{W,2}a_{L,1})$, and $c_3 = (a_{W,2}a_{L,3} - a_{W,3}a_{L,2})$.

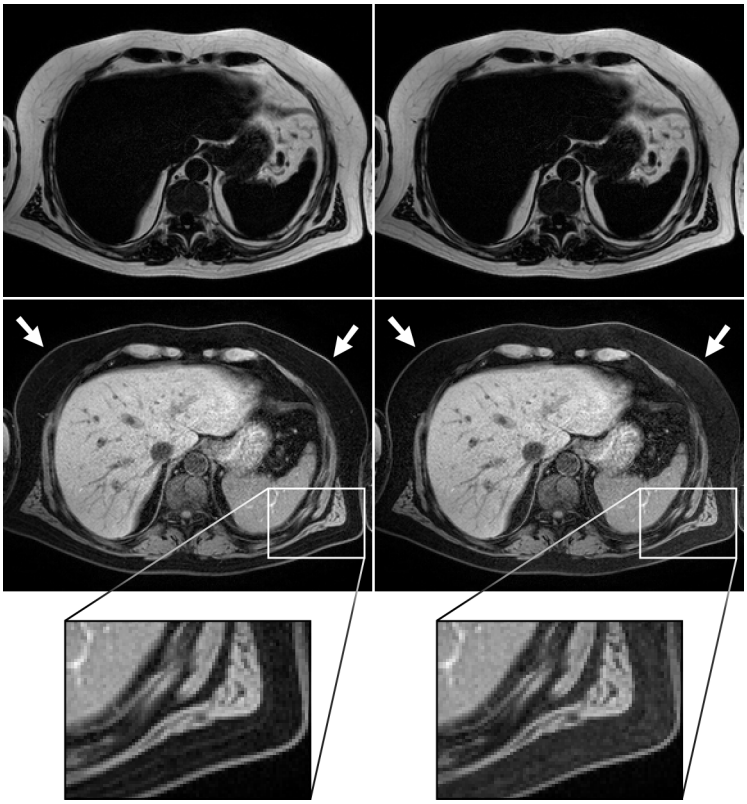

Fig. 1. Lipid (top) and water (bottom) images calculated using the simple signal model (right) and the advanced signal model (left). The advanced signal model results in stronger and more uniform fat suppression (arrows), and reveals more detail of the subcutaneous adipose tissue (zoomed box).

The ± ambiguity of eq. 3 is resolved under the assumption of spatial smoothness of the error phasor, for instance by a region-growing algorithm [4]. Finally, the least-squares estimates of *W* and *L* are given by eq. 4 with the matrix definitions given by eq. 5.

For demonstration, a 2D multi-gradient-echo abdominal image was obtained during a single breath-hold, from a healthy volunteer who gave informed consent, using a 1.5 T clinical MR scanner (Achieva, Philips Healthcare, Best, the Netherlands) and a 16-channel phased array torso coil. FOV: 375 × 298 mm, acquired voxelsize: 1.4 × 1.4 × 8 mm, reconstructed matrix: 288 × 228, $TE_1/\Delta TE/TR$: 3.1/2.7/80 msec, FA: 80°, BW: 515 Hz/pixel, breath-hold time: 17.4 sec.

The reconstruction was implemented in MATLAB on a standard laptop computer, for both the simple spectrum model (single lipid peak and no relaxation) and the advanced model, where numerical values of α, $\Delta\omega$, and R_2 were taken from the literature [5]. For comparison, the reconstruction was also performed using Levenberg-Marquardt optimization with a maximum of ten iterations per voxel.

$$S_n = (a_{W,n}W + a_{L,n}L)\exp(i\omega_0\Delta t)^{n-1} \quad [1]$$

$$\begin{aligned} a_{W,n} &= \exp(-TE_n R_{2,W}) \\ a_{L,n} &= \textstyle\sum_{p=1}^{P} \alpha_p \exp(i\Delta\omega_p t_n - TE_n R_{2,p}) \end{aligned} \quad [2]$$

$$\exp(i\omega_0\Delta t) = \frac{S_2c_1 \pm \sqrt{S_2^2c_1^2 - 4S_1S_3c_2c_3}}{2S_1c_3} \quad [3]$$

$$\begin{bmatrix} W_{\mathrm{LS}} & L_{\mathrm{LS}} \end{bmatrix}^T = \left(\mathbf{A}^H\mathbf{A}\right)^{-1}\mathbf{A}^H\mathbf{S} \quad [4]$$

$$\mathbf{S} = \begin{bmatrix} S_1 & S_2/\exp(i\omega_0\Delta t) & S_3/\exp(i\omega_0\Delta t)^2 \end{bmatrix}^T$$
$$\mathbf{A} = \begin{bmatrix} a_{W,1} & a_{W,2} & a_{W,3} \\ a_{L,1} & a_{L,2} & a_{L,3} \end{bmatrix}^T \quad [5]$$

Results The calculation of separate water and lipid images from the complex triple-echo images took 0.25 sec for the closed-form solution and 141 sec for the optimization. The water and lipid images obtained with the simple and the advanced spectrum models are shown in fig. 1. The advanced model gives better fat suppression in the water image.

Discussion In practice, R_2 values vary with tissue. Yet, the proposed signal model is more general than the conventional, where it is implicitly assumed that R_2=0. The presented closed-form solution is simple and saves processing time, compared to optimization. It can also be used as an initial guess for optimization if the number of points exceeds three. Accurate lipid spectrum modeling potentially gives better fat suppression compared to single-peak modeling.

References **1.** Dixon WT. Radiology 1984;153:189–194. **2.** Yu H et al. Magn Reson Med 2008;60:1122–1134. **3.** Xiang QS, An L. J Magn Reson Imaging 1997;7:1002–1015. **4.** Berglund J et al. Magn Reson Med 2010;63:1659–1668. **5.** Hamilton G et al. Proc ISMRM 2010:4726.